Experimental study of transient paths to the extinction in sonoluminescence

Raúl Urteaga, Damián Dellavale, Gabriela F. Puente, and Fabián J. Bonetto
Laboratorio de Cavitación y Biotecnología, Instituto Balseiro-CAB-CONICET, R8402AGP–Av. Bustillo Km. 9,5–San Carlos de Bariloche-Río Negro, Argentina

(Received 5 June 2007; revised 2 January 2008; accepted 6 March 2008)

An experimental study of the extinction threshold of single bubble sonoluminescence in an air-water system is presented. Different runs from 5% to 100% of air concentrations were performed at room pressure and temperature. The intensity of sonoluminescence (SL) and time of collapse (t_c) with respect to the driving were measured while the acoustic pressure was linearly increased from the onset of SL until the bubble extinction. The experimental data were compared with theoretical predictions for shape and position instability thresholds. It was found that the extinction of the bubble is determined by different mechanisms depending on the air concentration. For concentrations greater than ~30%–40% with respect to the saturation, the parametric instability limits the maximum value of R_0 that can be reached. On the other hand, for lower concentrations, the extinction appears as a limitation in the time of collapse. Two different mechanisms emerge in this range, i.e., the Bjerknes force and the Rayleigh–Taylor instability. The bubble acoustic emission produces backreaction on the bubble itself. This effect occurs in both mechanisms and is essential for the correct prediction of the extinction threshold in the case of low air dissolved concentration. © *2008 Acoustical Society of America.* [DOI: 10.1121/1.2903854]

PACS number(s): 43.35.Hl [AJS] Pages: 1490–1496

I. INTRODUCTION

Sonoluminescence is the phenomenon where a pulsed light source is obtained from an ultrasonic field. Given that the light belongs to the visible spectra, a concentration of 12 orders of magnitude in energy density is obtained.[1] This phenomenon occurs when a bubble is trapped in an antinode pressure (velocity node) of a standing wave. When the pressure amplitude is increased, the bubble oscillations become highly nonlinear and produce a violent collapse. During the collapse, an almost adiabatic heating of the inner gas is achieved, leading to the thermal emission process.[1,2]

The region of the parameter space in which this phenomenon occurs is limited by two main factors. First, the collapse must be strong enough to produce the necessary heating of the bubble contents. This implies that the point in the phase diagram must be above the Blake threshold.[3] Second, the bubble must remain stable during the whole process. In addition to the diffusive and chemical stabilities, which determine the equilibrium position in the phase space, the shape and position stability must be satisfied, i.e., the bubble must not break into pieces and it has to remain trapped in the pressure antinode.

Holt and Gaitan[4] and Gaitan and Holt[5] studied the stability boundaries of single bubble sonoluminescence (SBSL). They found that two upper limits appear. One limit is in the ambient radius (R_0) and the other is in the acoustic pressure (P_a) in which stable SBSL is obtained.

The upper threshold in R_0 has been interpreted as the onset of the parametrical instability, in reasonable accordance with the experimental data.[5–8] This limit extends to the region where the bubble is not sonoluminescent. However, regarding the limit in P_a, there is a controversy as to which mechanism is responsible for the extinction.[9]

In addition, the experimental data collected in the region of the SBSL parameter space by most groups[4–7] have been obtained in static conditions of acoustic pressure. In this way, the points in the vicinity of extinction are inaccessible because they are, in general, unstable.

The instability in the vicinity of the extinction threshold is associated with a recycling mode.[4,5,10,11] Furthermore, it has been divided into two types depending on the temporal pattern. Type 1 is associated with a sudden drop in intensity and time of collapse, followed by a slow increase of both quantities in the order of seconds. Type 2 is similar to type 1, but the maximum intensity is tenfold smaller and has a colder spectrum than stable sonoluminescence (SL).[10] Those modes of recycling are related to a bubble pinch off and formation of multiple fragments. These fragments can dissolve or recombine to form a new bubble with a renewed intake of air. In type 1 recycling, the nitrogen and oxygen are burned off while the equilibrium diffusive concentration is reached. In type 2, instead, the instability threshold is reached before the burn off becomes efficient and, therefore, the bubble is mostly air filled.[10]

Dam and Levinsen[10] observed that both types of recycling modes are preceded by a period doubling in the amplitude of SL. This fact and the spatial anisotropy in the flashes are indications that the instability would be instigated by a nonspherical perturbation. In addition, An *et al.*[9] calculated the instability threshold of SL under a nonspherical symmetrical acoustic pressure perturbation. They chose this perturbation as a parameter to fit the available experimental data without specifying the source of such a perturbation.

Besides, Holzfuss and Holt[12] showed that the shock wave emitted by the bubble generates a complex mode field consisting of higher harmonics of the applied driving. These

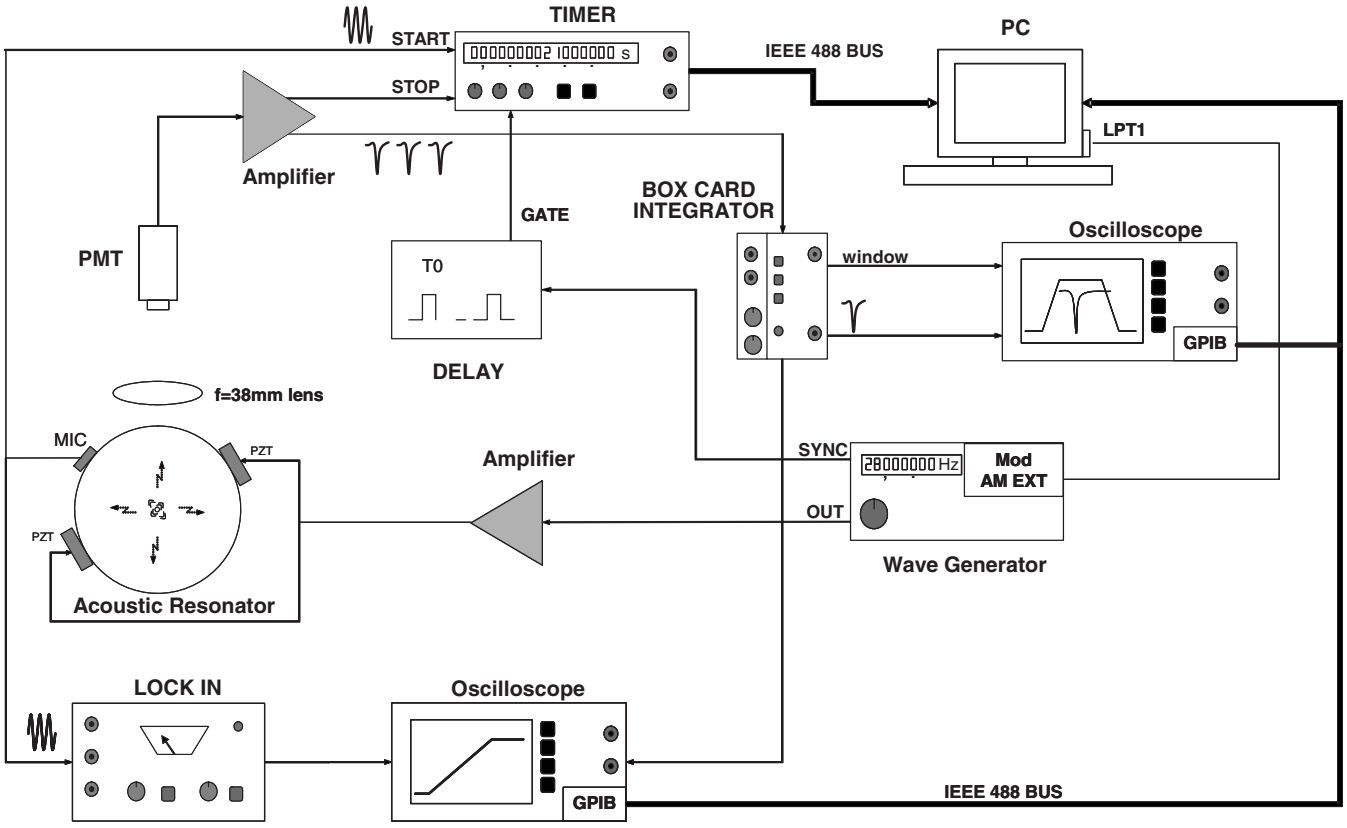

FIG. 1. Experimental setup. Typical apparatus for SBSL in which a driving voltage ramp is applied. The SL intensity, microphone signal, and time of collapse are acquired as a function of time.

harmonics extend to the megahertz range and have about 10% of the driving amplitude. Holzfuss and Holt found that the bubble position and stability are determined by this complex sound field.

In this work, we measure the data points in phase space in a continuous way by slowly increasing the acoustic pressure. As a consequence, we can access the region close to the extinction. Repetitions of these experiments give us an indication of the statistical occurrence of the extinction threshold. Moreover, we can explore the region in which the dynamics are unstable and obtain an estimation of the strength of instability.

The results are compared with theoretical predictions of the extinction threshold for different instabilities of shape and position. A close relationship between the extinction and the high frequency harmonics emitted by the bubble is proposed.

II. APPARATUS

Measurements were made by using a typical apparatus for SBSL similar to the one first reported in Ref. 8. We use a Pyrex made spherical resonator 60 mm in outer diameter with a resonance frequency of approximately 28.3 kHz. The resonator cell was filled with distilled, 0.45 μm filtered, and partially degassed water. After filling, the liquid sample was sealed to prevent diffusion to the atmosphere. The experiments were conducted at a controlled temperature of 23 °C and a room pressure of 0.92 bar. The whole setup was thermally isolated and temperature controlled. We surveyed the phase space of SBSL by making a continuous increase in the voltage of the drivers from the onset of SL until the extinction of the bubble for a set of different concentrations of dissolved air. The air concentrations were between 5% and 100% with respect to the saturation. To determine the position in the phase space at each moment, we simultaneously measured the time of collapse (defined as the time between the zero crossing of acoustic pressure with negative slope and the bubble collapse), the SL flash intensity, and the microphone signal.

Figure 1 shows the experimental setup. A function generator signal was amplified by an audio amplifier and a resonant *RLC* circuit. In such a circuit, the capacitance was the piezodrivers (PZT) of the resonator. The output of the function generator was computer controlled to generate the amplitude-modulated wave for the resonator driving.

In each run, the frequency was adjusted to the resonant frequency of the system. The resonant frequency changes indicate the slight increase in temperature because of the piezodriver heating.

We linearly increased the acoustic pressure from the onset of SL, at about 1.2 bar, until the bubble extinction at about 1.4 bar. To choose the acoustic pressure increase rate, two facts must be taken into account. First, the rate of increase must be small enough to ensure a negligible departure from the behavior under a constant acoustic pressure at each instant. On the other hand, the rate of the increase must be as high as possible to explore the unstable extinction region. In

order to satisfy these constraints, we choose approximately 4 mbar/s for the acoustic pressure increase rate (i.e., each run takes about 50 s).

The pressure values at the beginning and end slightly depend on the particular dissolved air concentration. In all the runs, the pressure increase rate was the same.

We measured the SL pulse intensity using an Oriel 33740 phototube (PT). We obtained the bubble time of collapse and the SL intensity from the PT signal. A small piezoelectric crystal (microphone) was glued to the resonator wall to obtain a signal proportional to the applied acoustic pressure. The time of collapse was measured with a Stanford Research timer (SR620). The timer start and stop signals were obtained from the microphone and PT pulse, respectively. The time precision of the measurements was only limited by the microphone signal jitter (about 50 ns). The timer was operated at its maximum rate of about 1200 samples/s, which is close to $\frac{1}{24}$ of the resonator frequency.

The microphone signal was filtered by a lock-in amplifier referenced to the function generator output. Thus, a signal proportional to the resonator driving amplitude was obtained. The integration time of the lock-in was 10 ms in all the measurements.

A gated integrator boxcar Stanford Research Systems (SRS) averages the intensity of 1000 samples of the SL flash at a frequency of about 14 kHz (half of the driving frequency). The lock-in output and the SL intensity were acquired by a digital oscilloscope connected via General Purpose Instrumentation Bus (GPIB) to the computer.

Another digital oscilloscope was used to monitor the integrator window (3 μs in width) and the SL pulse coincidence in time. The SL pulse was preamplified 25 times by using a Stanford Research amplifier (SR244). Hence, the PC acquired the time of collapse, the microphone, and the SL intensity as a function of the measurement time.

The temporal evolution of the bubble radius was measured using the Mie scattering technique (not shown in Fig. 1)[8,13–15] at different acoustic pressure values for each air dissolved concentration. In these measurements, the values of acoustic pressure were constant in time.

We use the numerical model described in Ref. 8 to fit the bubble radius temporal evolution. We outline here the different components of our model. See Ref. 8 for more details. The model includes the following: (1) transient and spatially nonuniform heat transfer using a collocation point method, dissociation of O_2 and N_2, and mass diffusion of vapor in the noncondensable gases inside the bubble; (2) nonequilibrium evaporation and condensation of water and a temperature jump due to the accommodation coefficient at the bubble interface; and (3) transient and spatially nonuniform heat transfer using a collocation point method and mass diffusion of the gas in the liquid. The model computes the gas diffusion in the liquid and inside the bubble following a similar approach to the one used for the thermal equation by obtaining the points in phase space that are stable from a mass diffusive point of view.[16] The chemical kinetic model describes the molecular decomposition of the water vapor molecules inside the bubble upon collision with an inert gas. It includes the elementary reactions between stable species and free radicals for the system.

The acoustic pressure obtained from the model was used to calibrate the filtered microphone signal. A calibration of the microphone was made for each dissolved air concentration. The calibrations do not show statistical variation for the different air concentrations.

The ambient radius (R_0) was computed by the numerical model[8] from the acoustic pressure and time of collapse values. We take R_0 at the time when the acoustic pressure is zero with negative slope. We want to remark that, while it is well established that the determination of acoustic pressure with this technique is quite good (0.05 bar precision),[1,8,15] the value of R_0, instead, will be correctly predicted only in case a chemical and diffusive equilibrium inside the bubble is developed.

Finally, it is important to note that because of the measurement system, based on the detection of the flash pulses, the parameter space obtained is strictly for sonoluminescence.

III. RESULTS

Figures 2(a)–2(c) show the time of collapse, the SL intensity, and the microphone signal, respectively, as functions of the measurement time in an experimental run. The air concentration was about 5% with respect to saturation. We set the bubble extinction time as $t=0$ s.

In this particular experiment, the ramp was started at $t=-30$ s, increasing the driving signal amplitude until the bubble extinction at $t=0$ s.

The time of collapse, the SL intensity, and the microphone signal amplitude mean values monotonically increase. However, several fluctuations appear in the whole range, as is shown in Fig. 2. At a time of about −8 s, a different behavior arises with particular features until the extinction of the bubble.

The bursts observed in Fig. 2(a) at times $t=-20$ s and $t=-14$ s (details in the insets) were common in all the measurements regardless of the air concentration. The particular shape and temporal position of the burst were different for each measurement. However, for a given air concentration, the ramp zones where the time of collapse has low variance are quite repetitive. This fact will be further analyzed from the results of Fig. 3.

Figure 2(a), insets 1 and 2, show that the time of collapse fluctuations are quite complex. In some cases (inset 2), the structure is similar to the period doubling reported in the past.[17] Time of collapse fluctuations as those displayed by inset 1 have not been reported in the literature.

The SL intensity [Fig. 2(b)] decreases in coincidence with the time of collapse burst. At higher acoustic pressures and before the bubble extinction, a series of sudden drops in time of collapse appears. At the same time, a tenfold decrease in SL intensity is observed. This behavior is similar to the one investigated by Dam and Levinsen[10] and named the second recycling mode. In Ref. 10, a period doubling is found just before that recycling mode appears. We are not

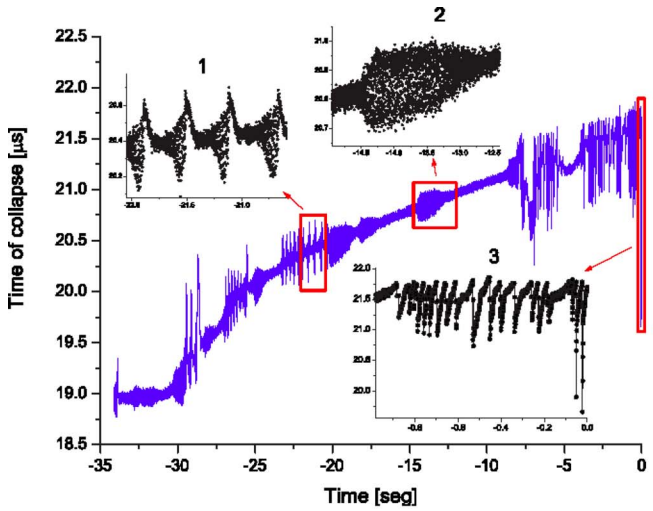

(a)

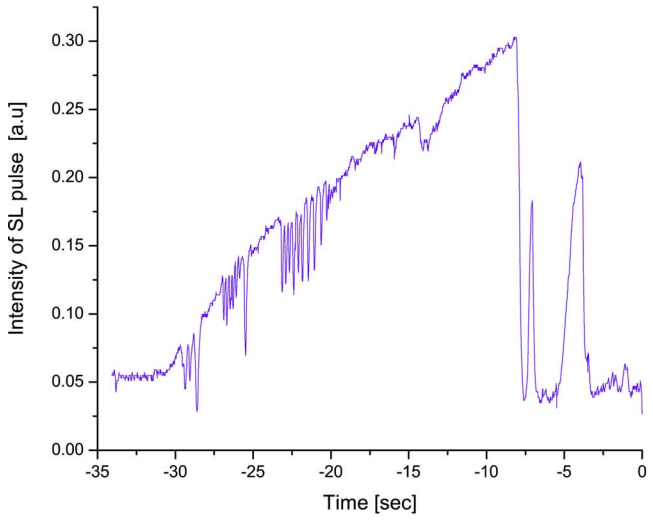

(b)

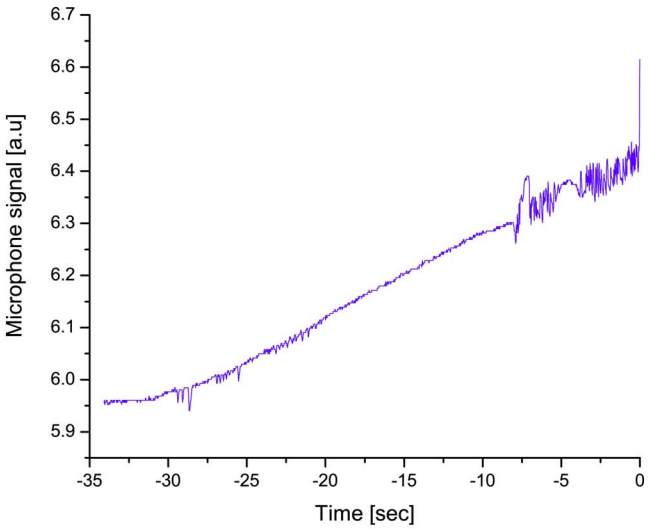

(c)

FIG. 2. (Color online) (a) Time of collapse temporal evaluation for 5% dissolved air with respect to saturation. The insets show details of fluctuations and the extinction. (b) Light pulse intensity for the same run as in (a). The intensity results from a running average of 1000 pulses. (c) Driving frequency component of the microphone signal.

able to detect this feature because of the running average performed by the boxcar integrator in the SL intensity determination.

Two stability regions can be recognized from Fig. 2, at times $t=-7$ s and $t=-4$ s. In those regions, the time of collapse is almost constant and the SL intensity slowly increases. Note that the slow increase is not an integration effect but a diffusive process within the bubble. The drops, instead, seem to be limited only by the SL pulse integration.

Figure 2, inset 3, shows an enlargement of the final stages of the bubble before the extinction. In such a region, the occurrence frequency of recycling is quite high (30–100 Hz). In the last stage, the amplitude of recycling also increases and the bubble suddenly disappears.

Figure 3 shows the SL intensity as a function of measurement time for six realizations at ~5% of air concentration with respect to saturation. The SL intensity monotonically increases with the time of collapse almost until the bubble extinction.

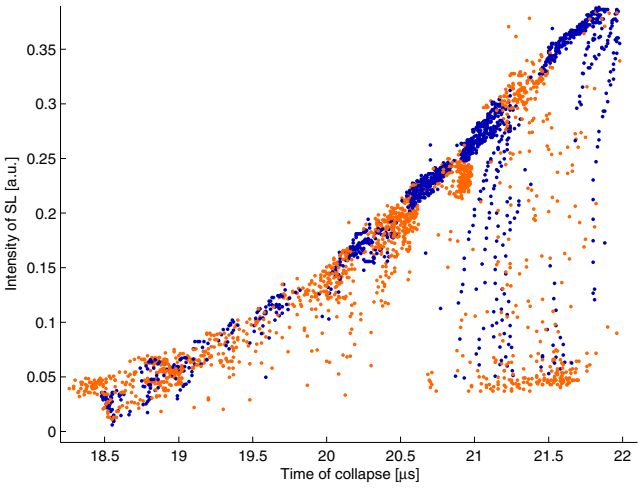

FIG. 3. (Color online) The SL intensity measured during the ramp in voltage of PZT for six runs at ~5% of air concentration with respect to saturation as a function of time of collapse. Stable (black dots, blue online) and unstable (gray dots, red online) points are separated. It is considered stable if the maximum difference at the time of collapse of 500 consecutive points is lower than 150 ns.

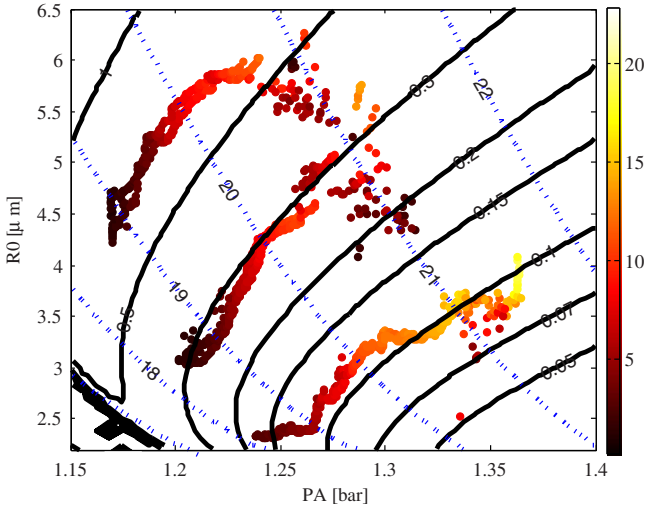

FIG. 4. (Color online) Phase diagram of sonoluminescence. The points are the experimental results for three different air concentrations (from bottom to top: 0.14, 0.4, and 0.5, respectively). For each air concentration, two runs are shown. The gray level (color online) maps the SL intensity relative to the scale at the right. The filled black lines are the equilibrium curves for different air concentrations. The dashed (blue online) lines are the constant time of collapse curves.

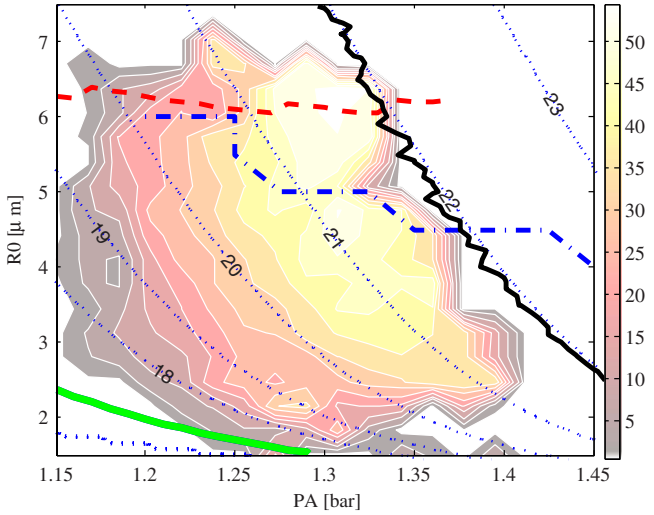

FIG. 5. (Color online) Phase space of sonoluminescence. The thin dashed (blue online) lines are the constant time of collapse curves. The thick dashed (red online) line is the parametric instability for the mode $n=2$ (Refs. 1 and 8); the dotted dashed (blue online) line is the Rayleigh–Taylor instability for the mode $n=2$ (Refs. 1 and 8); the filled gray (green online) line is the Blake threshold. The filled black line is the Bjerknes force threshold where a high frequency harmonic of the acoustic pressure has been taken into account in the calculation.

However, before the bubble extinction, the SL intensity presents a decrease until values as low as 10% of the maximum SL intensity. The decrease in SL intensity is coincident with the second recycling mode in the last stage of Fig. 2.

In Fig. 3, "stable" and "unstable" points are classified. This differentiation was obtained by computing the maximum time of collapse difference among 500 consecutive points. When that difference was bigger than 150 ns, the points were considered unstable; otherwise, they were considered stable.

Figure 3 shows separated zones for stable and unstable points especially at high acoustic pressure values. Also, the stability islands of Fig. 2 correspond to stable point region of Fig. 3. The ambient radius (R_0) and acoustic pressure (P_a) were computed from the measured time of collapse and microphone signal, respectively.

Figure 4 displays the R_0 and P_a values for three different air concentrations (the measured values of C_{inf}/C_0 were 0.14, 0.4, and 0.5). To illustrate the measurement fluctuations, two runs are shown for each air concentration. The SL intensity is mapped into the color bar at the right of Fig. 4.

The assigned errors of the points are 50 ns for the time of collapse (t_c) and 0.05 bar for the acoustic pressure (P_a). The acoustic pressure errors at high air dissolved concentrations are larger (0.1 bar) due to the relatively poor bubble spatial stability. The ambient radius error is determined by the P_a and t_c errors and the position in the phase diagram. The R_0 error is bounded to 0.7 μm for small R_0 values and 1.5 μm for high R_0 values.

As Fig. 4 shows, the SL intensity monotonically increases with the acoustic pressure for the three air concentrations. Nevertheless, a region of low SL intensity for times of collapse at about 21 μs can be observed. This region corresponds to the low SL intensity points at the right of Fig. 3. Figure 4 shows that the measured values of air concentration reasonably agree with the ones predicted by the numerical model. While the pathways for $C_{\text{inf}}/C_0=0.4$ and 0.5 follow the trends of the equilibrium curves, the path for $C_{\text{inf}}/C_0=0.14$ shows a more pronounced deviation at low acoustic pressure.

For measured air concentrations higher than 60%, the points lie on stability curves of lower calculated air concentrations. For measured air concentrations of 82% and 100%, the points were always unstable and spread over the whole phase diagram around the time of collapse curve of 21 μs.

Figure 5 displays R_0 and P_a values for 11 air concentrations in the range of 5%–100%. About ten runs in each concentration were measured. To adequately represent the high number of data points, the SL intensity was averaged into patch regions of 0.08 μm and 6 mbar over the whole phase diagram. The SL intensity is mapped into the color bar at the right of the figure.

Figure 5 shows that the SL intensity increases with the acoustic pressure for all air concentrations. Besides, it is worth noting that the SL intensity seems to be determined only by the time of collapse value, regardless of the air concentration.

In Fig 5, other than the stable equilibrium and time of collapse curves, the calculated parametric instability, Rayleigh–Taylor instability, and Bjerknes instability threshold are also included. In order to close the phase space of SL, the Blake threshold is included. The Bjerknes instability was calculated by taking into account two acoustic field contributions: The first component was the acoustic field generated by the drivers at the frequency of resonance (f_{res}) and the second contribution was an 11-fold in frequency and a 10% in amplitude with regard to the first contribution. The relative phase between them was set to zero. At $t=0$ the fundamental crosses zero with negative slope ($-\sin(2\pi f_{\text{res}}t)$). We define

the relative phase equal to zero when at $t=0$ the harmonic (second contribution of the acoustic field) crosses zero with negative slope too. Similar results were obtained by considering another harmonic. On the other hand, the phase between the harmonics is a sensitive parameter. We chose the phase in order to obtain the calculated extinction threshold for the smallest time of collapse value.

With regard to the extinction threshold, it can be observed that for calculated concentrations higher than 30%, the extinction of the bubble is determined by an upper value in equilibrium radius. This fact is in good accordance with the limit set by the parametric instability.

For calculated air concentrations lower than 30%–40%, we found that the evolution of SL presents an upper limit in the time of collapse between 21.5 and 22 μs.

The Rayleigh–Taylor instability calculated as in Ref. 8 is not consistent with the threshold established by the experimental data.

IV. DISCUSSION

From the onset of SL at low acoustic pressure, the light emission process is stable except for the existence of zones in which burst in time of collapse appears [Fig. 2(a), insets 1 and 2]. The positions of those zones are reproducible in different runs for a fixed air dissolved concentration and temperature. These bursts present a complex structure. In some cases, a period doubling and even more sophisticated evolutions were observed.

With the exception of some earlier works,[5,12] these interesting structures have been largely overlooked in SL. We believe that it is because the bursts are experimentally obtained only in small regions and present a high sensitivity upon the control parameters such as temperature or dissolved gases.

At higher acoustic pressures and before the extinction, a recycling mechanism is developed [Fig. 2(a), inset 3]. It is possible to recognize two types of recycling modes that differ in the recycling frequency and SL intensity. In Fig. 2(a), a zone of the first mode is developed between regions of the second recycling mode at the end of the temporal evolution.

The first recycling mode was predominant at high air concentrations and appears at lower acoustic pressure values than the second type. We found that the extinction of the bubble always occurs after the second recycling mode is developed, regardless of the air concentration (Fig. 4). The measurement time (i.e., the range of acoustic pressures) that the bubble persists in the second recycling mode increases with the dissolved air concentration; as a matter of fact, for air saturated water, the bubble is in a recycling mode in the whole range of acoustic pressures where SL is observed.

We interpret the extinction as a statistical event in which each pinch off of the bubble in the recycling mode is a potential extinction. We experimentally found that the extinction probability is a function mostly of the time of collapse of the bubble. This is true for air concentration lower than 30%–40%. For higher concentrations, the parametric instability seems to be the mechanism that produces the extinction.

Taking into account the characteristics of the recycling mode, specifically, the existence of a period doubling in SL amplitude and correlated spatial anisotropy,[11] and the pinch off of the bubble in fragments,[10,11] we associated the onset of this phenomenon to a nonspherical acoustic pressure perturbation.

We perform a simple analysis of the intensity of ultrasound emitted by the bubble from the temporal evolution of the radius (from the numerical model).[3] The results show that the total emission of ultrasound also mainly depends on the time of collapse. This preliminary calculation is not conclusive but gives us an indication that a possible source for the perturbation is actually the ultrasound emission of the bubble that interacts with the resonator. Furthermore, there is evidence[12,15,18,19] that the ultrasound emission of the bubble affects the position and stability of the bubble.

In the calculated instability threshold of SL by An *et al.*[9] a nonspherical symmetrical acoustic pressure perturbation is utilized as a parameter to fit the available experimental data without specifying the source of such a perturbation. However, the calculated threshold shows the correct dependence at low air dissolved concentrations.

On the other hand, we present the results on the Bjerknes instability when an acoustic harmonic is considered. This calculation does not pretend to evaluate the exact value of the Bjerknes force from the complete ultrasonic field that experiences the bubble but evaluates the reliability of the mechanism. The stability threshold obtained fits rather well the experimental data. Nevertheless, it is worth noting that the stability threshold does not imply the bubble extinction. In addition, if the Bjerknes force is the mechanism that limits the values of the time of collapse, it is expected that the SL intensity smoothly varies while the bubble goes away from the center of the resonator. This feature was never observed in the experiments.

V. CONCLUSIONS

We study the evolution of the SL while a continuous increase in acoustic pressure was applied. We found two different behaviors determined by the air dissolved concentration. For concentration higher than 40%–50% with respect to saturation, the extinction of the bubble is determined by an upper value in equilibrium radius. This fact is in good agreement with the limit set by the parametric instability.

For air dissolved concentrations lower than 30%–40%, we found that the evolution of SL presents a different mechanism for the extinction. We experimentally found that the extinction probability is a function mostly of the time of collapse value.

We propose two different mechanisms that could explain this behavior: A Rayleigh–Taylor instability amplified by a nonspherical acoustic perturbation and the existence of a destabilizing Bjerknes force that takes into account the contribution of the acoustic harmonics.

Although both mechanisms show the correct dependence, the mechanism of the nonspherical acoustic perturbation is more consistent with the experimental observation of an abrupt extinction of the bubble. However, more calcula-

tions including the measured value of the perturbations are necessary to validate the proposed mechanism. Nevertheless, in both mechanisms analyzed, the backreaction of the bubble acoustic emissions seems to be essential for the correct prediction of the extinction threshold for low air concentrations.

ACKNOWLEDGMENTS

The authors thank Daniel Mateos, Sebastián Eckardt, and Enrique Aburto for technical support. This work was funded by CONICET and CNEA.

[1]M. P. Brenner, S. Hilgenfeldt, and D. Lohse, "Single-bubble sonoluminescence," Rev. Mod. Phys. **74**, 425–484 (2002).
[2]Y. An and C. F. Ying, "Model of single bubble sonoluminescence," Phys. Rev. E **71**, 036308 1–12 (2005).
[3]T. G. Leighton, *The Acoustic Bubble* (Academic, London, 1994).
[4]R. G. Holt and D. F. Gaitan, "Observation of stability boundaries in the parameter space of single bubble sonoluminescence," Phys. Rev. Lett. **77**, 3791–3794 (1996).
[5]D. F. Gaitan and R. G. Holt, "Experimental observations of bubble response and light intensity near the threshold for single bubble sonoluminescence in an air-water system," Phys. Rev. E **59**, 5495–5502 (1999).
[6]J. A. Ketterling and R. E. Apfel, "Extensive experimental mapping of sonoluminescence parameter space," Phys. Rev. E **61**, 3832–3837 (2000).
[7]J. A. Ketterling and R. E. Apfel, "Shape and extinction thresholds in sonoluminescence parameter space," J. Acoust. Soc. Am. **107**, L13–L18 (2000).
[8]G. F. Puente, R. Urteaga, and F. J. Bonetto, "Numerical and experimental study of dissociation in an air-water single-bubble sonoluminescence system," Phys. Rev. E **72**, 046305 1–10 (2005).
[9]Y. An, T. Lu, and B. Yang, "Instability of sonoluminescing bubbles under a nonspherical symmetrical acoustic-pressure perturbation," Phys. Rev. E **71**, 026310 (2005).
[10]J. S. Dam and M. T. Levinsen, "Second mode of recycling together with period doubling links single-bubble and multibubble sonoluminescence," Phys. Rev. Lett. **94**, 174301 (2005).
[11]J. S. Dam, M. T. Levinsen, and M. Skogstad, "Stable nonspherical bubble collapse including period doubling in sonoluminescence," Phys. Rev. E **67**, 026303 (2003).
[12]J. Holzfuss and R. G. Holt, "Acoustical stability of a sonoluminescing bubble," Phys. Rev. E **66**, 046630 (2002).
[13]B. P. Barber and S. J. Putterman, "Light scattering measurements of the repetitive supersonic implosion of a sonoluminescing bubble," Phys. Rev. Lett. **69**, 3839–3842 (1992).
[14]B. Gompf and R. Pecha, "Mie scattering from a sonoluminescing bubble with high spatial and temporal resolution," Phys. Rev. E **61**, 5253–5256 (2000).
[15]T. J. Matula, S. M. Cordry, R. A. Roy, and L. A. Crum, "Bjerknes force and bubble levitation under single-bubble sonoluminescence conditions," J. Acoust. Soc. Am. **102**, 1522–1527 (1997).
[16]S. Hilgenfeldt, D. Lohse, and M. Brenner, "Phase diagrams for sonoluminescing bubbles," Phys. Fluids **8**, 2808–2826 (1996).
[17]R. G. Holt, D. F. Gaitan, A. A. Atchley, and J. Holzfuss, "Chaotic sonoluminescence," Phys. Rev. Lett. **72**, 1376–1379 (1994).
[18]J. Holzfuss, M. Ruggeberg, and A. Billo, "Shock wave emissions of a sonoluminescing bubble," Phys. Rev. Lett. **81**, 5434–5437 (1998).
[19]T. J. Matula, "Inertial cavitation and single-bubble sonoluminescence," Philos. Trans. R. Soc. London, Ser. A **357**, 225–249 (1999).